Natural Convection Driven Melting of Phase Change Material: Comparison of Two Methods

Farid Samara[1], Dominic Groulx[*1], and Pascal H. Biwole[2]
[1]Mechanial Engineering, Dalhousie University, Halifax, Nova Scotia, Canada,
[2]Department of Mathematics and interactions, University of Nice Sophia-Antipolis, France
*Corresponding author: PO Box 15000, Halifax, NS, Canada, B3H 4R2, dominic.groulx@dal.ca

Abstract: Latent heat energy storage systems (LHESS) are one potential technology that can be used to store thermal energy when there is a mismatch between time of production and time of utilization of such energy. Design of LHESS requires knowledge of the heat transfer process within them, as well as the phase change behavior of the phase change material (PCM) use. COMSOL Multiphysics can be used to model (LHESS), enabling testing of a multitude of configurations, as well as an optimization of the geometry used. Natural convection plays a crucial role during the charging phase of the LHESS (melting of the PCM), and methods to incorporate this heat transfer mode within COMSOL simulation of PCM melting have been underway for quite some time. This paper presents a comparison between two such related methods, which are both treating the PCM as a liquid regardless of its actual phase; but are using added function to "solidify" this liquid when the PCM is below its melting temperature. Tests were conducted using COMSOL Multiphysics 4.3 and a simple 2D geometry is used to perform the comparison. Although the first method presented is intuitive and simple to increment, it was found that the second method is more robust, stable and has a better convergence.

Keywords: Phase Change Heat Transfer, Melting, Natural Convection, Phase Change Material, Latent heat.

Nomenclature:

A	User defined function
B	User defined function
C	Arbitrary constant
C_p	Specific heat capacity (J/kg·K)
F	Force (N)
g	Gravity (m/s^2)
H	PCM container height (m)
k	Thermal conductivity (W/m·K)
l	Aluminum sheet thickness (m)
L	PCM container internal width (m)
L_f	Latent heat of fusion (kJ/kg)
MF	Melted fraction
P	Pressure (Pa)
t	Time (s or min or hour)
T	Temperature (K)
T_0	Initial temperature (K)
T_∞	Surrounding air temperature (K)
T_m	Melting temperature (K)
ΔT	Range of melt temperature
q	Arbitrary constant
$\vec{u}$	Liquid PCM velocity (m/s)
x	Cartesian coordinate (m)
y	Cartesian coordinate (m)
β	Thermal expansion Coefficient (1/K)
ρ	Density (kg/m^3)
μ	Dynamic Viscosity (Pa·s)

Subscript

b	Buoyancy
l	Liquid
s	Solid

1. Introduction

Latent heat energy storage system (LHESS) have the interesting characteristic that the phase change material (PCM) used in them has the capacity of storing up to 14 times more energy than most sensible heat storage over a relatively narrow temperature interval which encompasses the melting temperature of the PCM [1]. The amount of stored energy is simply proportional to the latent heat of fusion of the PCM. This makes LHESS an interesting technology to store thermal energy in systems when energy capture and utilisation do not coincide in time, for example, solar thermal and waste heat recovery in industrial processes [2].

LHESS are face with one major drawback: PCMs have extremely low thermal conductivities [3], which makes putting the energy in (melting) and extracting it (solidification) challenging in the sense that energy must be transferred in a timely manner that depends on the application.

One way of dealing with this constraint during the melting stage is to design LHESS in a

way that promotes natural convection, which as result speeds up the overall melting process by increasing the amount of heat transfer through the liquid PCM [4]. Numerical modelling can help in the design of such system, but methods that account for natural convection must be developed and tested first.

This paper presents two such methods, developing their mathematical and physical basis, and goes on to compare them. The next section will present the system, geometry and material used in the models and simulations. Section 3 will described both method and the meshes used during this work. Comparative results will be presented in section 4 followed by a conclusion.

2. System, Geometry and Material

The geometry used to perform the method comparison in this study is presented in Fig.1, and his based on a geometry of a solar photovoltaic (PV) collector initially used by Biwole *et al.* [5]. The PCM is enclosed in a box having a height H=0.132 m and a width L=0.02m, thermally insulated at the top and bottom. A sheet of aluminum of thickness l=0.004 m is placed on both sides of the PCM, as it would in a PV system, to ensure rapid heat transfer to the PCM.

As for initial and boundary conditions; the entire PCM is initially solid at room temperature, T_o = 293 K. At t = 0, a heat flux q''= 1000 W/m^2, representing absorbed solar radiation, is imposed on the outside left wall. Forced convection is also present on both outside walls with convection coefficient on the left and right wall of 10 W/m^{2}K and 5 W/m^{2}K respectively (T_∞=T_o).

RT25, a commercial PCM from Rubitherm GmbH, chosen for this study since it was also the material originally used by one of the author in previously published work [5]. Its thermophysical properties presented in Table 1 were manually input in COMSOL Multiphysics.

Table 1: Thermophysical Properties of RT25 [X]

	Cp (J/kg·K)	k (W/m·K)	ρ (kg/m^3)
Solid RT25	1800	0.19	785
Liquid RT25	2400	0.18	749
Aluminum	903	211	2675
Constant Properties of TR25			
L_F = 232000 J/Kg		T_m = 299.75 K	
β = 10^{-3} 1/K		μ=1.798 ×10^{-3} kg/m·s	

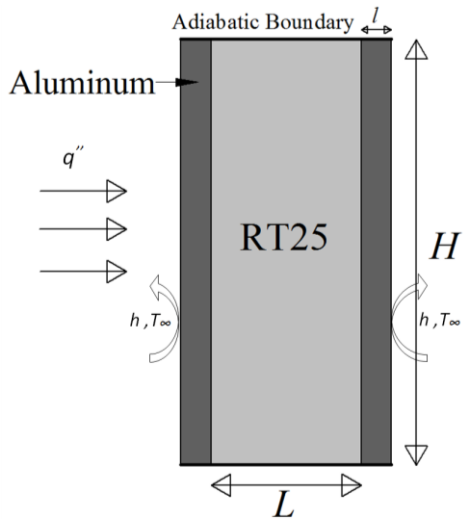

Figure 1. Problem geometry and boundary conditions.

3. Use of COMSOL Multiphysics

A 2D numerical study was performed in COMSOL Multiphysics 4.3 to simulate heat transfer and melting of the PCM found in the system previously presented. The model was created to account for both conduction heat transfer in the solid PCM and conduction/natural convection heat transfer in the liquid PCM. The following three physics were used to create the model: heat transfer in solids (aluminum), heat transfer in fluids (PCM) and laminar flow (PCM).

The previous three physics can easily simulate for heat transfer and buoyancy driven fluid flow as long as there is no phase change. In order for the COMSOL model to account for both the dynamic and energetic behavior of the PCM during its phase change, two methods have been used and are compared in this work. For each method, several material parameters, as well as mathematical variables/functions, had to be introduced.

3.1 First Method: Modified Viscosity

The first method used as been experimented with in the laboratory of one of the author, Groulx. In it, the following steps must be taken to account for phase change and the presence of natural convection in the liquid melt.

The large latent heat of fusion (L_f) absorbed by the solid PCM during melting is modeled using a modified specific heat (C_p), as presented by Eq.(1) [6]:

$$C_p(T) = \begin{cases} C_{ps}, & T < T_m \\ \frac{C_{ps}+C_{pl}}{2} + \frac{L_f}{\Delta T}, & T_m < T < T_m + \Delta T \\ C_{pl}, & T > T_m + \Delta T \end{cases} \quad (1)$$

where C_{ps} and C_{pl} are the solid and liquid PCM specific heat and ΔT is the temperature range over which the melting occurs. For this work, ΔT is selected to be 1 K.

Equation (1) is implemented in COMSOL Multiphysics by using a continuous second derivative function, this enable smoothing of the sudden changes in the PCM specific heat. The resulting $C_p(T)$ is presented in Fig. 2.

As a result, this modified specific heat, acting over the range of temperature T_m to $T_m+\Delta T$, accounts for both the latent heat and sensible energy. The area under the curve in Fig. 2 should be approximately equal to the latent heat of fusion, plus a minor contribution from the specific heat of the PCM. This modified specific heat method has been validated previously by comparing it to the classic Stephan problem [7].

In this method, the entire PCM is treated as a liquid, even when its temperature is lower than its melting point; a modified viscosity is used to force this liquid to behave as a solid when it has to. A piecewise, continuous, second derivative function centered about T_m is used to define the modified viscosity as follows:

$$\mu(T) = \begin{cases} 10^6, & x < T_m + \Delta T/2 \\ \mu_l, & x \geq T_m + \Delta T/2 \end{cases} \quad (2)$$

A solid PCM is then defined as a liquid having an extremely large viscosity, while the liquid PCM posses its true value μ_l when the PCM is melted. Figure 3 presents the PCM viscosity as a function of temperature.

Finally, a volume force must be added to the physics to simulate the buoyancy force giving rise to natural convection. The Boussinesq approximation is used to account for this buoyancy force, as shown in Eq.(3):

$$\overrightarrow{F_b} = \vec{g}\rho\beta(T - T_m) \quad (3)$$

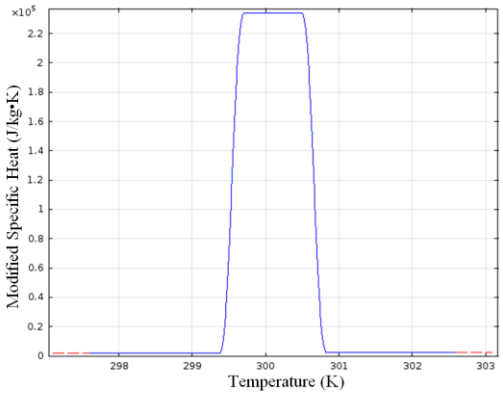

Figure 2. Modified specific heat.

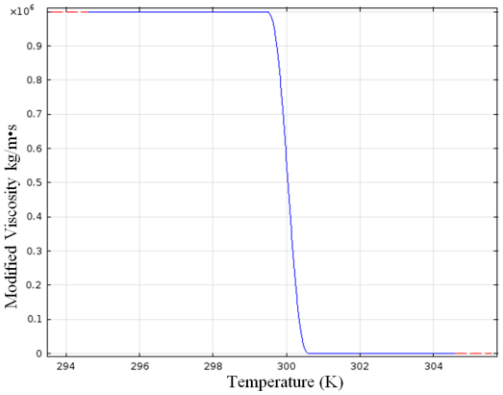

Figure 3. Modified dynamic viscosity.

This first method is relatively easy and straight forward to implement. The use of a modified viscosity to account for a immovable liquid below the melting point was shown to give physically meaningful results [8, 9]. However, the physical simplicity of the method sometimes leads to extremely long simulations, or simulations that simply cannot converge.

3.2 Second Method: Modified Volume Force

The second method used, which was used previously by Biwole *et al.* [5], goes deeper in the mathematical formulation of the functions required to account for phase change, but still represents the PCM as a liquid regardless of its temperature. Numerical solvers have an easier time handling functions that do not present large abrupt changes, like the ones shown in Figs. 2 and 3. For that reason, the modified heat capacity function used in this method is built around two smoother functions.

First, a Gaussian function, $D(T)$, is used to account for the latent heat over a melting temperature range ΔT. This function has a value of zero everywhere except over the interval (T_m - ΔT) to ($T_m+\Delta T$) centered at T_m. Most importantly, its integral is equal to 1, so by multiplying $D(T)$ by L_f, the energy balance is ensure for a simulation that starts at a temperature lower than (T_m – ΔT) and ends above ($T_m+\Delta T$). This function is presented in Eq. (5) and shown in Fig. 4:

$$D(T) = e^{\frac{-T(T-T_m)^2}{\Delta T^2}} \Big/ \sqrt{\pi \Delta T^2} \quad (4)$$

To account for the change in specific heat between the solid and the liquid phase of the PCM, a simple piecewise function $B(T)$ is created as shown in Eq.(5) and Fig. 5:

$$B(T) = \begin{cases} 0, & T < (T_m - \Delta T) \\ \frac{T - T_m + \Delta T}{2\Delta T}, & (T_m - \Delta T) < T < (T_m + \Delta T) \\ 1, & T > (T_m + \Delta T) \end{cases} \quad (5)$$

$B(T)$ is equal to zero for temperature lower than the melting point, and is equal to 1 after melting. It increases linearly from 0 to 1 over the melting temperature range ΔT.

It would be possible to smooth this function one step further in the future by getting rid of the sharp corners at both end of the linear stretch from (T_m -ΔT) to (T_m+ΔT). Similarly, even though the thermal conductivity and density of the liquid and solid PCM are not changing significantly, the function $B(T)$ is used to modify them as well, taking into account there small differences.

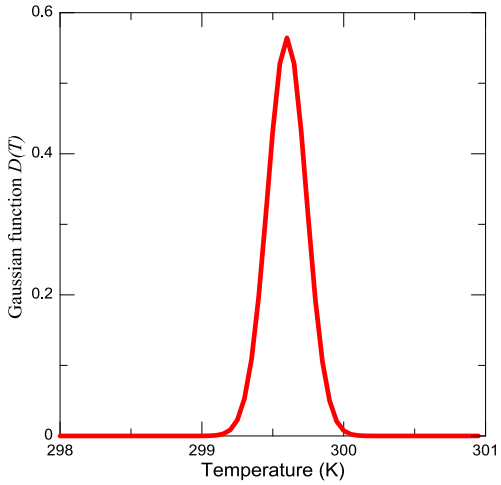

Figure 4. Gaussian function $D(T)$ used to account for the latent heat of fusion in a modified specific heat.

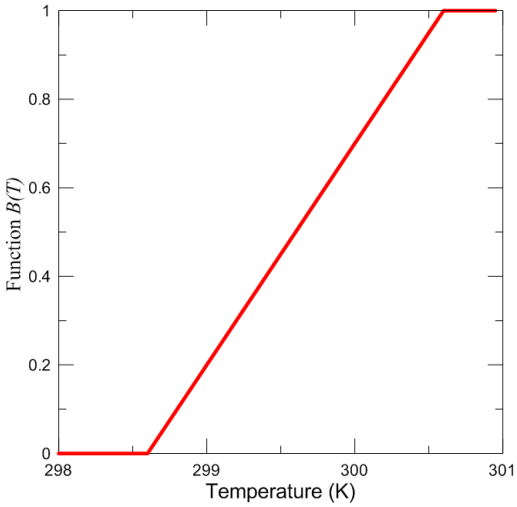

Figure 5. Function $B(T)$ used to account for the change in C_p, k, and ρ between the solid and liquid phase of the PCM.

To ensure a second order continuous function, $B(T)$ is represented by the flc2hs smoothed Heavside function in COMSOL Multiphysics as follows:

$$B(T) = flc2hs((T - T_m), \Delta T_m) \quad (6)$$

The following equations then define the thermophysical properties of the PCM:

$$\rho(T) = \rho_s + (\rho_l - \rho_s) \times B(T) \quad (7)$$

$$k(T) = k_s + (k_l - k_s) \times B(T) \quad (8)$$

$$C_p(T) = C_{Ps} + (C_{Pl} - C_{Ps})B(T) + L_F D(T) \quad (9)$$

A volume force is again added to the physics to simulate the effect of natural convection and also uses the Boussinesq approximation. Its form is slightly different than what was presented in Eq. (3), but the result is the same:

$$\overrightarrow{F_b} = -\rho_l(1 - \beta(T - T_m))\vec{g} \quad (10)$$

The major difference between the two methods can be found in function $A(T)$, define as follows:

$$A(T) = \frac{C(1 - B(T))^2}{(B(T)^3 + q)} \quad (11)$$

where C and q are arbitrary contants given the values of 10^5 and 10^{-3} respectively.

This function is equal to zero when the PCM is a liquid and is equal to 10^8 when the PCM is a solid as presented in Fig. 6. The slope of the transition zone starts off steep then diminishes at (T_m-ΔT/2).

$A(T)$ is first used to describe the viscosity function as follows:

$$\mu(T) = \mu_l(1 + A(T)) \quad (12)$$

where μ_l is the liquid PCM viscosity. By the definition of $A(T)$, the viscosity of the solid PCM is again pushed toward infinity. As the PCM changes phase to liquid, the value of $A(T)$ diminishes to zero, making $\mu(T) = \mu_l$.

As mentioned previously, the PCM is treated completely as a liquid which forces the Navier-Stoke equation to calculate the velocity everywhere, even when the PCM is a solid. This increases the number of calculations significantly and increases the chance the solver will diverge during the simulation (as it sometimes does when the first method is used). To quickly force

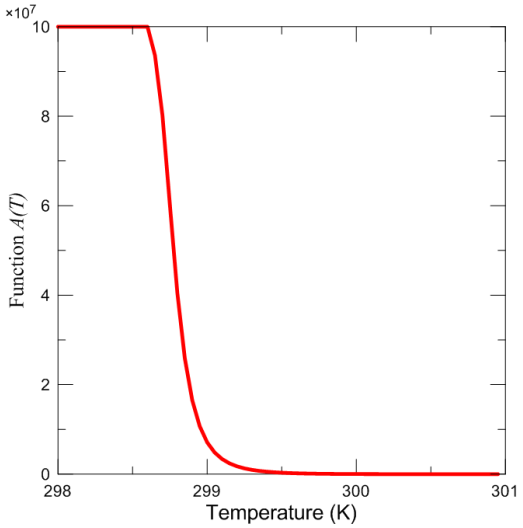

Figure 6. Function $A(T)$ used to define the viscosity function, and modify the volume forces found in the Navier-Stokes equation.

COMSOL Multiphysics to calculate velocities equal to zero in the solid PCM, a volume force ($\overrightarrow{F_a}$) is added to the Navier-Stoke equation:

$$\rho\frac{\partial\vec{u}}{\partial t}+\rho(\vec{u}.\nabla)\vec{u}-\mu.\nabla^2\vec{u}=-\nabla P+\overrightarrow{F_b}+\overrightarrow{F_b} \quad (13)$$

with

$$\overrightarrow{F_a}=-A(T)\cdot\vec{u} \quad (14)$$

The impact of $\overrightarrow{F_a}$ is to dominate every other force terms in the momentum equations when the PCM is solid, speeding up the calculation and effectively forcing a trivial solution of $\vec{u}$ = 0 in the solid.

This method is mathematically better define and introduces elements (smoother functions and modified Navier-Stokes equation in the solid phase) that should reduce the number of iterations taken by the solver.

3.3 Model Mesh

Two meshes were produced and used for the comparative simulations performed in this paper; they are presented in Fig. 7.

The first one uses quadrilateral elements. A mapped mesh was created by specifying the number of nodes along each side of the PCM. A boundary layer was added around the inner wall. Simulations were run using either 9200 or 18840 elements, since any more elements required simulation times of more than a week. Either linear or quadratic elements where used to discretize the temperature profiles. Simulations took an average of 5 to 7 days on an Intel Xeon Quad Core processor. A representation of this mesh is presented in Fig. 8.

The second mesh used free tetrahedral elements; 53679 elements were used to build this mesh which is presented in Fig. 9. Only linear discretization of the temperature where considered for this mesh.

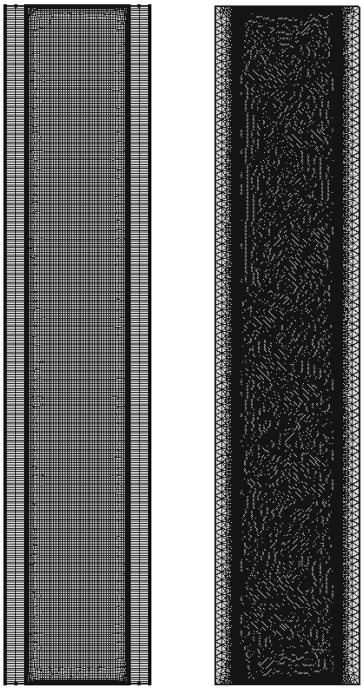

Figure 7. Two meshes used in this study; mapped mesh using quadrilateral elements with a boundary layer on the inside of each surface (left) and a free triangular Mesh (right).

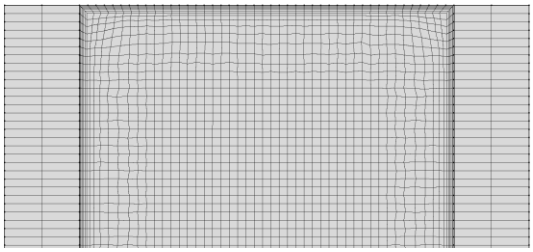

Figure 8. Quadrilateral mesh at the top-height cross section of the model.

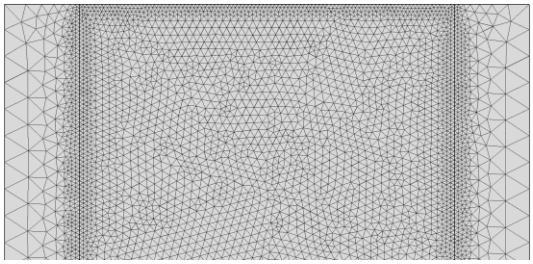

Figure 9. Free triangular Mesh at the top-height cross section of the model.

Table 2: Summary of the six model simulation to compare the two methods studied.

Model Number	Brief Description	Temperature Discretization	Number of Elements	Mesh Geometry	Boundary Layer	Total melting time	Number of iterations	Length of the Simulation
1	First Method	Linear	53924	Free Triangular	Around the inner wall	Diverged at 4200 sec		
2	Second Method	Linear	53678	Free Triangular	Around the inner wall	6060 sec	17483	160.6 hours
3	Second Method	Quadratic	9200	200 by 30 quadrilateral	On the left wall	7380 sec	41619	98 hours
4	Second Method	Linear	9200	200 by 30 quadrilateral	On the left wall	7560 sec (*MF*=96 %)	33226	16.5 hours
5	Second Method (force in Eq. (14) = 0)	Linear	53678	Free Triangular	Around the inner wall	6000 sec	17120	46.8 hours
6	Second Method	Quadratic	18840	300 by 45 quadrilateral	Around the inner wall	6630 sec	63874	296.75 hours

4. Results and Discussion

The two methods presented previously where tested on two different types of mesh, leading to six different model results, as presented in Table 2. The results of those six main simulations will be compared in lights of the obtained melting fraction of the PCM as a function of time and the progression of the melting interface as a function of time in the following two sub-sections.

4.1 Melting Fraction

Figure 10 presents the PCM melting fraction (*MF*), where a value of 0 means melting has not started yet, and 1 meaning the PCM is completely liquid.

The value of *MF* is obtained by performing a surface integration as per Eq. (15):

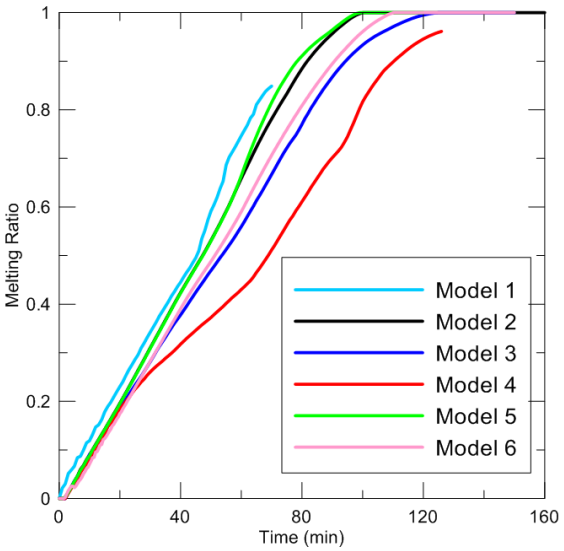

Figure 10. Melting fraction of different models versus time.

$$MF = \frac{\iint Area\ with\ (T>T_m)dxdy}{H \times L} \quad (15)$$

In Fig. 10, it can be seen that from zero to 35 minutes, all the models look similar to each other. This is because, at first, the dominant heat transfer mode conduction, and all the models simulate conduction in the same way. The effect of the mesh is also non-existent during those first 35 minutes. After 35 minutes, the dominant heat transfer mode transitions to natural convection. The effect of the mesh is first seen for model 4 (second method), which is the coarser mesh used, with linear discretization of the temperature. It can be seen that the amount of melting drastically slows down after 35 minutes. in that case.

Upon visual observation of the results, it was seen that the solid-liquid interface in model 4 was rougher, which also points to the fact that the mesh was too coarse for this type of simulation.

Model 3 is similar to the model 4, but uses a quadratic discretization instead of a linear one. It can be seen that this small change results in a much better trend for the melting fraction, although the melting seems to slow down slightly after 40 minutes. As a drawback, this increases the simulation time by a factor of 6.

In model 6, the amount of element is double compared to models 3 and 4. Even though it took 296 hours for the simulation to run, no noticeable slow down in the melting rate is observed. Also, the shape of the solid-liquid interface is greatly defined as can be seen in Fig.11.

Models 2 and 5 both used a triangular mesh which contained more than five times the

number of elements found in models 3 and 4. They again use the second method. The melting fraction obtained for both models shows a nearly constant rate of melting. The solid-liquid interface is also very well defined upon visual inspection as can be seen in Fig. 12. The only difference between models 2 and 5 is that in model 5, the added force (Eq. (14)) in the Navier-Stoke equation (Eq. (13)) was removed. The total melting time was similar for both models, but the shape of the solid-liquid interface showed some difference over time which can be inferred from the small difference in the melting fraction observed after 60 minutes. The bigger difference was in the total simulation time; removing the added force in the model resulted in a reduction in the simulation time of a factor of 3.5.

Finally, the result of using the first method is show on model 1. This model started off with a higher melting rate than the other models. The melting faction obtained followed a trend similar to the other models; however, the simulation diverged after 75 minutes. This points out to the unstable nature of the first method under certain conditions.

4.2 Temperature Profile Comparison

Figures 11 and 12 present the temperature profiles at different times (30, 60, 75, 90 and 120 minutes), for model 6 and 2 respectively. The white line in those figures shows the solid-liquid interface. Those two models were selected to compare the best simulation results obtained with both types of mesh.

It can be seen from the two figures that melting was quicker in model 2. Also, it seems that the resulting curvature of the solid PCM during melting (see the top of the solid PCM at 75 minutes) is more pronounced in model 2, which uses smaller triangular elements, than in model 6 which used bigger quadrilateral elements.

4.3 Velocity Profile Comparison

Figures 13 and 14 present the amplitude and direction of the velocity inside the liquid PCM (red arrows) at different times (30, 60, 75, 90 and 120 minutes), for model 6 and 2 respectively. The blue line now shows the solid-liquid interface. It can be seen that, as expected, when the liquid PCM touches a hot surface, the aluminum in this case, buoyancy forces carries it upward. And when it touches a cooler surface, solid PCM or cold aluminum, it moves downward.

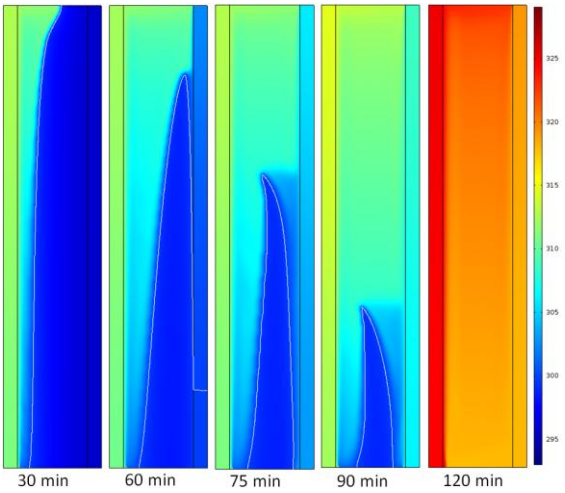

Figure 11. Model 6 temperature profiles for t = 30, 60, 75, 90, 120 min.

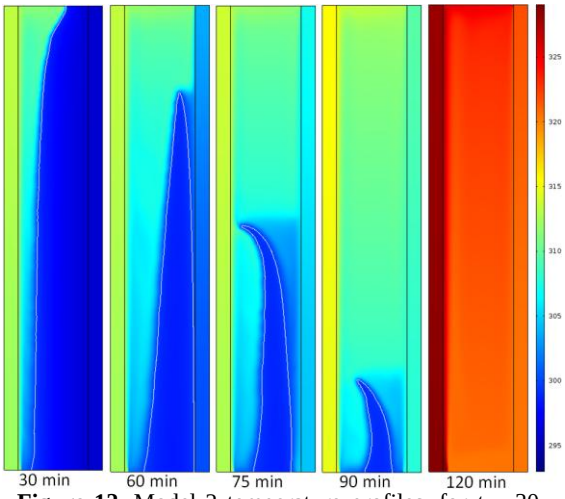

Figure 12. Model 2 temperature profiles, for t = 30, 60, 75, 90, 120 min.

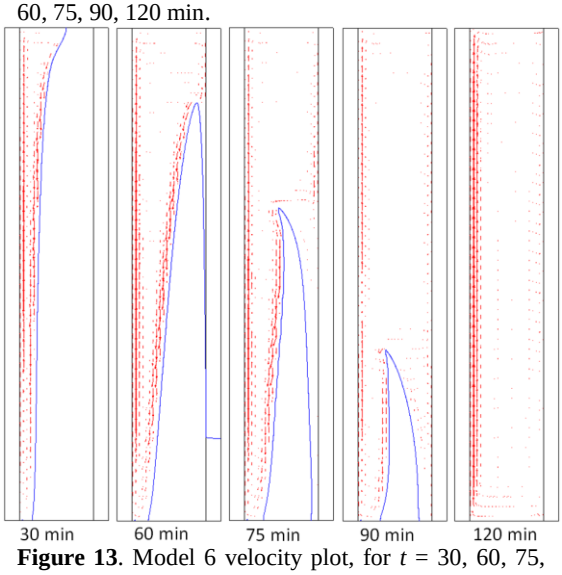

Figure 13. Model 6 velocity plot, for t = 30, 60, 75, 90, 120 min.

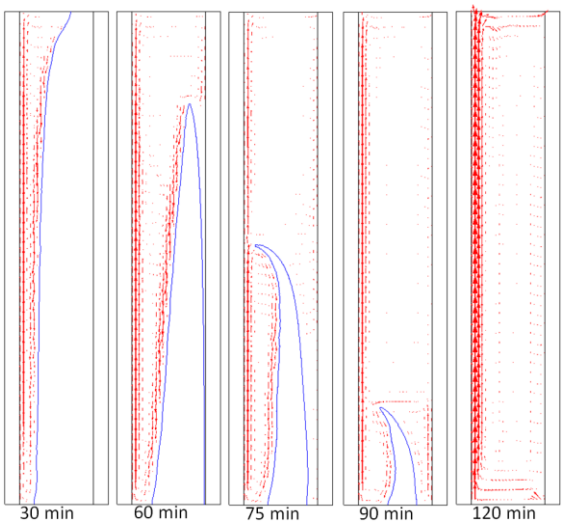

Figure 14. Model 2 velocity plot, for t = 30, 60, 75, 90, 120 min.

It appears that the velocity, hence the strength of natural convection, is higher in model 2; which explains why it is found that melting is simulated quicker in this model. It is also interesting that, as melting progresses, two circulation zone are created on either side of the remaining solid PCM as can be seen after 75 minutes, and is more pronounced after 90 minutes.

5. Conclusions

Two methods enabling the simulation of PCM melting while accounting for both conduction and natural convection have been presented and compared. It was found that the first method, which simply uses a modified viscosity, could properly simulate the phase change process only for part of the simulation, and diverge before reaching the end of the simulation.

The second method, which is more robust and uses smoother functions to account for changes in viscosity and specific heat, provide good consistent results.

The mesh used and discretization level of the temperature (linear or quadratic) have a strong impact on the overall simulated melting behavior and the obtained shape of the solid-liquid interface, as well as on the total simulation time.

Surprisingly, it was found that removing the extra body force term introduce in the second method to force the Navier-Stokes equation to quickly return a trivial answer for the velocity of the solid reduced the simulation time.

Still, in order to differentiate between the various results obtained here, an experimental validation should be performed.

6. References

1. Sharma, A., V.V. Tyagi, C.R. Chen, and D. Buddhi, Review on thermal energy storage with phase change materials and applications, *Renewable and Sustainable energy reviews*, **13**, p. 318-345 (2009)

2. Mehling, H. and L.F. Cabeza, *Heat and Cold Storage with PCM*, Springer, Berlin (2002)

3. Mills, A., M. Farid, J. Selman, and S. Alhallaj, Thermal conductivity enhancement of phase change materials using a graphite matrix, *Applied Thermal Engineering*, **26**, p. 1652-1661 (2006)

4. Liu, C., R.E. Murray, and D. Groulx, Experimental Study of Cylindrical Latent Heat Energy Storage Systems Using Lauric Acid as the Phase Change Material, *ASME 2012 Summer Heat Transfer Conference*, Rio Grande, Puerto Rico, USA, 10 p. (2012)

5. Biwole, P., P. Eclache, and F. Kuznik, Improving the Performance of Solar Panels by the use of Phase-Change Materials, *World Renewable Energy Congress 2011*, Linköping, Sweden, 8 p. (2011)

6. Groulx, D. and W. Ogoh, Solid-Liquid Phase Change Simulation Applied to a Cylindrical Latent Heat Energy Storage System, *COMSOL Conference 2009*, Boston, USA, 7 p. (2009)

7. Ogoh, W. and D. Groulx, Stefan's Problem: Validation of a One-Dimensional Solid-Liquid Phase Change Heat Transfer Process, *COMSOL Conference 2010*, Boston, USA, 6 p. (2010)

8. Liu, C. and D. Groulx, Numerical Study of the Effect of Fins on the Natural Convection Driven Melting of Phase Change Material, *COMSOL Conference 2011*, Boston, USA, 7 p. (2011)

9. Murray, R.E. and D. Groulx, Modeling Convection during Melting of a Phase Change Material, *COMSOL Confenrece 2011*, Boston, 7 p. (2011)

7. Acknowledgements

The authors are grateful to the Natural Science and Engineering Research Council of Canada (NSERC), to the NSERC CREATE Dalhousie Research in Energy, Advanced Materials and Sustainability (DREAMS) program and the Canadian Foundation for Innovation (CFI) for their financial assistance.